WILEY IWJ

ORIGINAL ARTICLE

# Cellular interactions with bacterial cellulose: Polycaprolactone nanofibrous scaffolds produced by a portable electrohydrodynamic gun for point-of-need wound dressing

Mehmet Onur Aydogdu[1] | Esra Altun[1] | Maryam Crabbe-Mann[2] | Francis Brako[2] | Fatma Koc[3] | Gunes Ozen[4] | Serap Erdem Kuruca[5] | Ursula Edirisinghe[6] | CJ Luo[2] | Oguzhan Gunduz[1] | Mohan Edirisinghe[2]

[1]Department of Metallurgical and Materials Engineering, Marmara University, Istanbul, Turkey

[2]Department of Mechanical Engineering, University College London (UCL), London, UK

[3]Department of Medical Microbiology, Medipol University, Istanbul, Turkey

[4]Department of Molecular Medicine, Istanbul University, Istanbul, Turkey

[5]Department of Physiology, Istanbul University, Istanbul, Turkey

[6]Accident and Emergency Department, St Mary's Hospital, London, UK

**Correspondence**
CJ Luo, PhD, Department of Mechanical Engineering, University College London (UCL), Torrington Place, London WC1E 7JE, UK.
Email: chaojie.luo@ucl.ac.uk

Electrospun nanofibrous scaffolds are promising regenerative wound dressing options but have yet to be widely used in practice. The challenge is that nanofibre productions rely on bench-top apparatuses, and the delicate product integrity is hard to preserve before reaching the point of need. Timing is critically important to wound healing. The purpose of this investigation is to produce novel nanofibrous scaffolds using a portable, hand-held "gun", which enables production at the wound site in a time-dependent fashion, thereby preserving product integrity. We select bacterial cellulose, a natural hydrophilic biopolymer, and polycaprolactone, a synthetic hydrophobic polymer, to generate composite nanofibres that can tune the scaffold hydrophilicity, which strongly affects cell proliferation. Composite scaffolds made of 8 different ratios of bacterial cellulose and polycaprolactone were successfully electrospun. The morphological features and cell–scaffold interactions were analysed using scanning electron microscopy. The biocompatibility was studied using Saos-2 cell viability test. The scaffolds were found to show good biocompatibility and allow different proliferation rates that varied with the composition of the scaffolds. A nanofibrous dressing that can be accurately moulded and standardised via the portable technique is advantageous for wound healing in practicality and in its consistency through mass production.

**KEYWORDS**
bacterial cellulose, electrohydrodynamic, electrospinning, polycaprolactone, wound dressing

## 1 | INTRODUCTION

Nanofibrous meshes or scaffolds have gained significant attention as a health care material over the last 2 decades for their considerable potential to facilitate tissue healing.[1,2] One of the promising application areas is wound dressing and implants. An ideal wound-healing material should protect the wound against infection but also provide a moist environment to enhance cell growth, efficient gas exchange, and high liquid absorption of physiological secretions and tuneable, tissue-specific nano- and micro-scale morphology and mechanical strength to direct cellular behaviour at the wound site.[3]

Cellulose is the most abundant biocompatible fibrous material on earth. Bacterial cellulose (BC) is a natural, non-toxic biopolymer commonly synthesised by *Gluconacetobacter xylinus*. Compared with plant cellulose, BC possesses higher water-holding capacity, higher purity and crystallinity, and exceptional mechanical strength. These properties make BC an excellent scaffold material for wound-healing

applications, including bone, cartilage, dental, skin, and muscle regeneration.[4–6] BC is commonly investigated as a scaffold as native BC fibrils or hydrogels of pure or composite materials.[7] BC nanofibres directly harvested from the bacteria or reconstituted hydrogels suffer from batch-to-batch variations. Hence, a problem for scaffold applications using this type of native BC is that it is hard to modulate cellular interactions with the BC fibres because of the lack of means to control the diameter, morphology, structure, and porosity of the native BC material. One way to solve the problem is to regenerate the raw BC fibres as man-made scaffolds using a method that can precisely control the nanofibre properties produced.

The synthetic production of an ideal 3D porous scaffold tailored for the varying needs of different wound-healing sites requires the optimization of a large range of material and processing parameters, including chemical, physical, and mechanical properties as well as features such as hydrophilicity and biodegradation rate.[8] Electrospinning is a well-known technique for its versatile ability to produce bespoke scaffolds that can be tailored to mimic a diverse range of extracellular environment for tissue regeneration.[9] As an electrohydrodynamic (EHD) process, it applies a strong electric field (kilovolt range) to rapidly generate fibres in the micrometre to nanometre dimension from a large library of liquid bulk materials.[10] The electrospun micro/nanofibrous scaffolds can promote haemostasis, fluid absorption, cell respiration, and gas permeation when implanted onto open wounds.[11] A major advantage of the EHD process is that the technique generates very uniform and near-monodisperse nanofibrous products, making it highly reproducible and reliable for health care applications.

However, native BC does not readily electrospin to form continuous, near-monodisperse nanofibres because of the poor solubility of cellulose in common organic solvents. Polycaprolactone (PCL) is a well-known thermoplastic polymer for EHD processing and is widely used in tissue-engineering applications. Its advantageous properties include good solubility in a broad range of common solvents, biocompatibility, bioresorbability, high mechanical strength, and tuneable viscoelasticity to tailor for different mechanical requirements.[12] In addition, PCL has been used in combination with other biopolymers such as gelatin[13] and mussel adhesive protein[14] to produce electrospun scaffolds with encouraging wound-healing results. However, PCL is made from petrochemicals and is therefore not a sustainable biomaterial; its hydrophobic nature also compromises its cytocompatibility and the ability to provide sufficient moisture and absorb fluid secretions at the wound site.[15] Hence, to exploit the advantages of BC and PCL as biomaterials for wound dressing, and to enable better control over the morphology and structure of the scaffold, we blend BC with PCL of 8 different ratios and use electrospinning to generate composite BC–PCL nanofibrous

**Key Messages**

- A portable electrospinning device was employed to produce at the point-of-need composite nanofibrous scaffolds for wound dressing applications.
- The portable apparatus eliminates the storage and transportation concerns with regards to the delicate nature of electrospun nanofibers, thereby preserving product integrity at the site of use while enabling the scaffolds to be applied to the wound site in a time-dependent fashion as demanded by the wound healing process.
- Composite nanofibrous scaffolds made of eight different ratios of bacterial cellulose and polycaprolactone were electrospun successfully for the first time.
- The composite scaffolds showed good biocompatibility and offer the advantage to tune the scaffold hydrophilicity, which strongly affects cell attachment and proliferation.

meshes. We study the cell proliferation in the samples and observe good biocompatibility.

Furthermore, we use a novel electrospinning device developed by Edirisinghe et al., named the "electrohydrodynamic gun" or "EHD gun," to generate the nanofibre scaffolds used here.[16,17] The distinct advantage of the EHD gun is its portable and hand-held convenience for nanofibre fabrication at the point of need. A major difficulty in the real-life application of nanofibres for the health care industry is the highly delicate nature of the nanofibrous products, making it difficult to package and transport the nanomaterial to the point of need. Conventional EHD apparatus to electrospin nanofibres are large and heavy, commonly fixed to the bench top in laboratories. They are not suitable for portable use in a non-laboratory environment. In contrast, the EHD gun can be hand-held or mounted for on-site use in places such as hospitals and ambulances, enabling the delicate nanofibrous materials to be applied directly to the wounded site, thereby ensuring that the nano-formulations are delivered intact to the wound site while saving valuable time to treatment.

## 2 | EXPERIMENTAL SECTION

### 2.1 | Materials

BC in pellet form was provided by the Department of Medical Microbiology, Medipol University (Istanbul, Turkey) and used as received without pretreatment. Poly($\varepsilon$-caprolactone) (PCL, Mw 80 000 g mol$^{-1}$), chloroform (CHCl$_3$), and dimethyl formamide (DMF) were obtained from Sigma-Aldrich (St. Louis, MO, USA). All reagents were of analytical grade and were used as received.

**TABLE 1** The contents of the samples S1–S8

| 50:50 wt ratio | 5% PCL | 10% PCL | 15% PCL | 20% PCL |
| --- | --- | --- | --- | --- |
| 5% BC | S1 | S2 | S3 | S4 |
| 10% BC | S5 | S6 | S7 | S8 |

BS, bacterial cellulose; PCL, polycaprolactone.

## 2.2 | Preparation of blended solutions

Solutions of PCL with varying concentrations (5, 10, 15, and 20 wt%) were prepared by dissolving an appropriate amount of PCL in DMF:CHCl$_3$ (50:50 weight ratio). The solutions were stirred using magnetic stirrers for 4 hours at 50 °C until complete dissolution of PCL. The 5 and 10 wt % BC were first dispersed in DMF using a homogeniser (Branson Ultrasonic Sonifier S-250A, Fisher Scientific, UK) for 30 minutes. Various concentrations of BC dispersions and PCL solutions were subsequently blended at 50:50 weight ratios, as shown in Table 1. The samples were stirred on a magnetic stirring plate at an ambient temperature of 23 °C for 2 hours and designated as samples S1–S8.

## 2.3 | Fabrication of nanofibrous scaffolds

A schematic drawing of the EHD gun used to produce the nanofibrous scaffolds is shown in Figure 1. The portable EHD gun was assembled with a single extrusion needle (Stainless tube & Needle Co. Ltd, Staffordshire, UK) of 0.69 mm inner diameter and 1.07 mm outer diameter and connected to a syringe containing the fibre-forming liquid. A strong potential difference was applied between the needle and a grounded collector using a high voltage supply (FC30 P4 12 W, Glassman Europe Limited, Bramley, UK). The working distance between the EHD gun needle exit and the grounded collector was set to 130 mm. The flow rates of the liquid were controlled using an ultra-high precision syringe pump (Infuse/Withdraw PHD 4400 Hpsi programmable syringe pump, Harvard Apparatus Ltd, Edenbridge, UK).

The syringe was of 10 mL capacity and loaded with solution samples S1–S8 (Table 1) to systematically study the nanofibres produced from liquids of varying BC:PCL contents. Nanofibres were collected on non-stick paper for 60 minutes. The applied voltage was optimised for each sample to obtain a stable cone-jet, an operating condition required for reproducible and uniform nanofibre formation by electrospinning. Parameters of the experiments are summarised in Table 2.

## 2.4 | Characterisations

Prior to electrospinning, the liquid properties of the samples S1–S8 were characterised by measuring their surface tension, viscosity, density, and electrical conductivity. Surface tension was measured using a calibrated force tensiometer (Biolin Scientific, Sigma 703D). Viscosity was measured using a programmable rheometer (Brookfield DV-III ULTRA, Harlow, UK). Density was measured using a standard density bottle (5 mL). Electrical conductivity was measured using a conductivity meter (Jenway 3450, Bibby Scientific Limited, Staffordshire, UK). All measurements were taken at ambient temperature and relative humidity (23 °C and 40–50%, respectively). The mean and standard deviation of 3 successive measurements were recorded in Table 3. All equipment were calibrated with ethanol.

Scanning electron microscopy (SEM) was carried out using a JEOL JSM-6301F operated at an accelerating voltage of 5 kV to determine the morphology and diameter of the fabricated nanofibres and cell–nanofibre interactions at 24 hours. Samples were coated with a thin layer of gold for 60 seconds using Quorum Q1500R ES (Quorum Technologies Ltd., UK). The diameters of the BC–PCL nanofibres were measured using image visualisation softwares: Image-J (NIH, USA) and Olympus AnalySIS 5 (Olympus, USA).
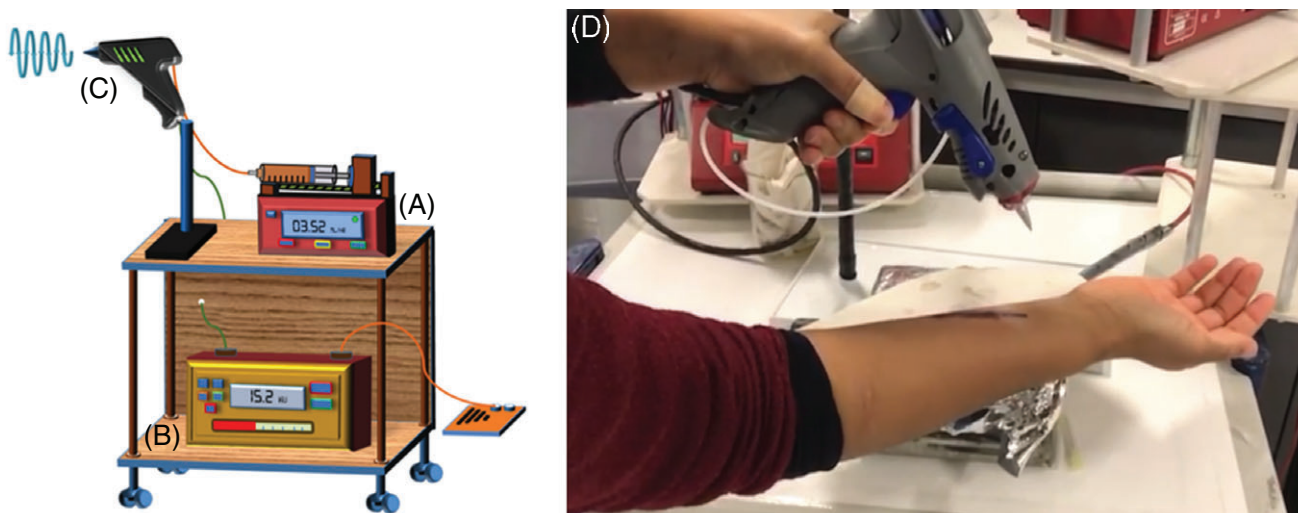


**FIGURE 1** A–C, A schematic drawing of EHD experimental setup: (A) syringe pump, (B) high voltage supply and (C) hand-held EHD gun. (D) a snapshot of the hand-held EHD gun treating a mock wound in real time

**TABLE 2** Summary of the processing conditions

| Sample/parameter | S1 | S2 | S3 | S4 | S5 | S6 | S7 | S8 |
|---|---|---|---|---|---|---|---|---|
| Voltage (kV) | 28.0 | 28.0 | 29.4 | 28.8 | 28.8 | 28.2 | 28.6 | 28.8 |
| Flow rate (mL h⁻¹) | 2 | 2 | 3 | 4 | 2 | 1 | 1 | 4 |
| Working distance (mm) | 130 | 130 | 130 | 130 | 130 | 130 | 130 | 130 |

Fourier transform infrared spectroscopy (FTIR, JASCO 6600, Japan) was used to confirm the presence of BC and PCL in the composite fibres by analysing the functional groups of the polymers in the as-spun nanofibres. A resolution of 4 cm⁻¹ at 32 scans and a range of 500–4000 cm⁻¹ were used.

The swelling characteristics of the scaffold samples S1–S8 were determined by immersing the samples in phosphate-buffered saline (PBS) solution at pH 7.4 for 24 hours at 37 °C. The swollen scaffolds were removed at specific time intervals (30, 60, 120, 180, 240, 300, and 1440 minutes) and weighed after removal of excess surface water using filter paper. The swelling percentage (SP) was calculated using equation: $SP = (W_w - W_d)/W_d \times 100$, where $W_w$ is the swollen weight, and $W_d$ is the dry weight of the scaffold sample. The 5 wt% PCL scaffolds were used as the control for reference.

Saos-2 cell line (*Homo sapiens* bone osteosarcoma, ATCC HTB-85) was used for cell viability assays. Scaffold samples were cut to 1 cm² sizes to fit into 96-well cell culture plates and sterilised overnight by UV irradiation. After cell seeding, samples were maintained in DMEM (Dulbecco's modified Eagle's medium, Sigma), supplemented with 10% foetal bovine serum (Sigma), penicillin (100 units mL⁻¹, Sigma), and streptomycin (100 g mL⁻¹, Sigma) at 37 °C in a 5% $CO_2$ humidified atmosphere. MTT (3-[4,5-dimethylthiazol-2-yl]-2,5-diphenyl-tetrazolium bromide) assay was used to assess cellular metabolism in the samples, and any potential cytotoxicity of the scaffolds. MTT assay provides a sensitive quantification of the number of viable cells in proliferation as reflected in the purple staining intensity acquired at the end of the analysis.[18] For MTT assay, Saos-2 cells were cultured for 72 hours in 96-well plates with 104 cells per 100 µL in each well containing scaffold samples. The control group comprised the same cell suspension of the same density per well in 96-well plates without the presence of scaffolds. After treatment, 10 µL of MTT reagent (5 mg mL⁻¹, Sigma) was incubated in the wells for 3–4 hours in darkness. The medium was then discarded, and the insoluble formazan crystals that formed were dissolved with 200 µL dimethyl sulfoxide. Finally, the absorbance values were read using ELISA plate reader (Rayto, China) at 570 nm, according to the 620 reference wavelength. All experiments were repeated at least 3 times.

For SEM imaging of the cell-seeded scaffolds, the scaffold samples prior to cell seeding were sterilised overnight by UV irradiation. Cells were then seeded on the surface of the samples at an approximate density of 106 cells per well in 6-well plates. Cell cultures were maintained for 24 hours and fixed with 2.5% glutaraldehyde. The samples were subsequently dehydrated in graded series of alcohol (30–100% ethanol in PBS) for 15 minutes each and left to dry. The scaffolds were stored at −20 °C until SEM imaging.

## 3 | RESULTS

The EHD technique is governed by processing parameters, including flow rate and the electric field strength, and material properties of the working solution, including polymer concentration, surface tension, viscosity, density, and electrical conductivity.[19] Controlling the relevant parameters leads to different EHD jetting modes,[20] with the stable cone-jet mode being the most desirable for robust and reproducible fibre formation. By optimising the flow rate and the electric field (the applied voltage over the distance between the charged electrode and the grounded electrode) as shown in Table 2, stable EHD cone-jets were obtained for each fibre-forming liquid sample. The physical properties of the samples S1–S8 are presented in Table 3. The polymer concentrations of PCL in the samples had a dominant influence on the physical properties of the solutions, as reflected by the increasing surface tension and viscosity and decreasing electrical conductivity when comparing sample group S1–S4 and S5–S8, in which the concentration of BC were respectively kept constant at 5 and 10 wt%, while the PCL concentration systematically increased from 5 to 20 wt% (Tables 1 and 3). SEM characterisations of the morphology of BC–PCL nanofibres revealed that increasing BC content from

**TABLE 3** Physical properties of the solutions used in experiments followed by standard deviation values (±)

| Sample name | Surface tension (mN m⁻¹) | Viscosity (mPa s) | Density (kg m⁻³) | Electrical conductivity (10⁻⁴ S m⁻¹) |
|---|---|---|---|---|
| SI | 30.8 ± 1.5 | 291.2 ± 7.1 | 0.9 | 12.4 ± 1.01 |
| S2 | 42.0 ± 0.7 | 402.8 ± 8.7 | 0.9 | 11.1 ± 0.02 |
| S3 | 54.2 ± 0.9 | 7665 ± 130 | 1.1 | 10.6 ± 0.04 |
| S4 | 62.5 ± 1.5 | 26475.6 ± 41.0 | 1.1 | 9.8 ± 0.03 |
| S5 | 33.9 ± 0.9 | 489.2 ± 13.4 | 0.9 | 23.1 ± 0.1 |
| S6 | 43.8 ± 0.3 | 533.8 ± 8.0 | 1.0 | 20.5 ± 0.05 |
| S7 | 57.6 ± 1.1 | 15477.8 ± 42.4 | 1.0 | 18.4 ± 0.07 |
| S8 | 64.7 ± 1.3 | 17980.4 ± 142.2 | 1.2 | 18.3 ± 0.04 |
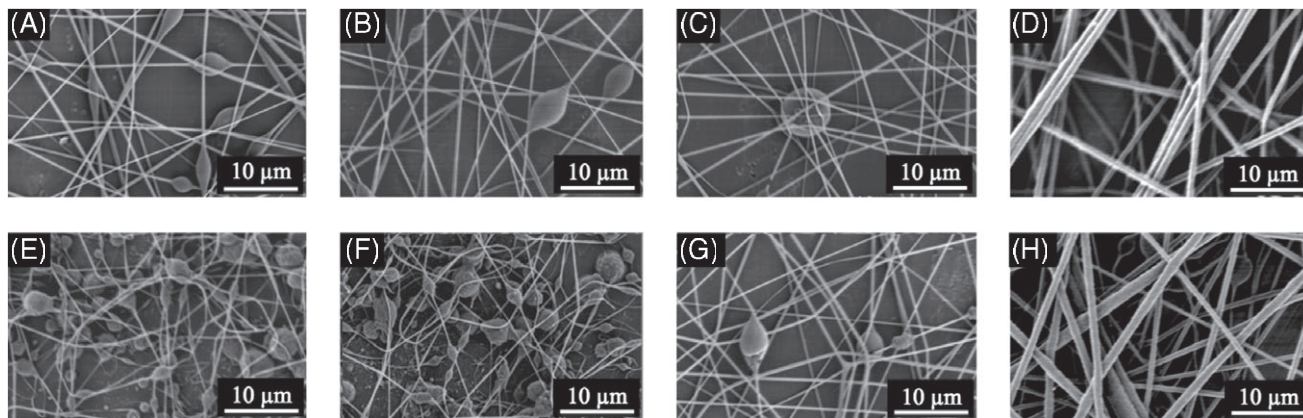
**FIGURE 2** Scanning electron micrographs of the samples: A, S1; B, S2; C, S3; D, S4; E, S5; F, S6; G, S7; and H, S8. Scale bars: 10 μm at 3000× magnification

5 to 10 wt% resulted in an amplified frequency of beaded fibres, while the increasing PCL concentration reduced the beading morphology and lead to electrospun smooth fibres at 20 wt% (Figure 2). The fibre diameter distribution profile (Figure 3) also showed a steady increase in the as-spun nanofibre diameter as PCL concentration increased in the samples (Table 1).

FTIR analysis confirmed the incorporation of PCL and BC in the composite nanofibres. Figure 4 shows a comparison of the FTIR spectra of pure BC, pure PCL, and the electrospun composite fibre samples S1–S8. The bands at 2900 and 1648 $cm^{-1}$ are assigned to the C–H stretching and the H–O–H bending of the absorbed water in the BC material; the band at 1060 $cm^{-1}$ is because of the C–O–C pyranose ring skeletal vibration of BC.[21] The absorption bands at 2940 $cm^{-1}$ are assigned to asymmetric stretching of the C–H groups; the bands at 2860 $cm^{-1}$ are assigned to symmetric stretching of the C–H groups; the bands at 1722 $cm^{-1}$ are assigned to C=O vibrations of the ester carbonyl group; the bands at 1238 $cm^{-1}$ are assigned to the asymmetric stretching of C–O—C of PCL.[22] Furthermore, the absorption peaks at 3343 and 1640 $cm^{-1}$ in the spectrum of pure BC have respectively shifted to 3304 and 1643 $cm^{-1}$ in the spectra of BC–PCL nanofibre samples, indicating interactions between the hydroxyl groups of BC and PCL in the BC–PCL composite fibres.

The Saos-2 cell culture results from the MTT assay at 72 hours are presented in Figure 5. A general increasing trend of cell viability was observed as PCL concentration increased from 5 to 20 wt%. The increase in PCL concentration corresponds to a steady increase in the electrospun fibre diameter, which we believe may have contributed to the different cell viability observed among the samples. Different cell types have been reported to prefer different fibre diameters for optimum attachment and proliferation. For example, oligodendrocytes prefer fibres with diameters above 400 nm and more preferentially 2–4 μm,[23] whereas fibroblasts show a reduction in cell attachment and proliferation when the fibre diameter increases from nanometre scale to micrometre

scale, possibly because nanofibres are more akin to the native extracellular condition of fibroblasts.[24] Moreover, using MC3T3-E1 mouse calvaria-derived osteoprogenitor cell line cultured on electrospun poly(lactic acid) fibres of 0.14–2.1 μm, Badami et al. observed increased osteoblast cell density with increasing scaffold fibre diameter.[25] Hence, the increasing Saos-2 cell viability, as observed with increasing PCL concentration is firstly attributed to the increasing fibre diameter among our samples. In addition, the lower fibre uniformity and presence of beading defects on scaffolds spun from lower PCL concentrations (samples S1–S3 and S5–S7) may have also unfavourably affected cell proliferation rates in these samples when compared with scaffolds with smooth, uniform fibres spun from 20 wt% PCL (S4 and S8).

Furthermore, the increasing trend of cell viability in sample groups S1–S4 (5 wt% BC) and S5–S8 (10 wt% BC) could also be because of the changing BC:PCL ratio as PCL concentration increased and BC concentration remained constant at 5 and 10 wt%, respectively. Interestingly, cells in the S4 sample with 5 wt% BC and 20 wt% PCL showed improved proliferation rate and higher metabolic activity when compared with cells seeds on scaffold S8, electrospun from 10 wt% BC and 20 wt% PCL. This indicated that the balance between BC and PCL ratio in the scaffolds affected cell viability. The combination of hydrophobicity and hydrophilicity changes as the BC:PCL ratio varied with changing BC and PCL concentrations.

The hydrophobicity of a synthetic material such as PCL can disrupt the initial cell adhesion behaviour.[26] By blending BC, a hydrophilic biopolymer, with PCL, a hydrophobic synthetic polymer, we aimed to improve the overall cytocompatibility of the composite material.[27] However, the cell viability in pure PCL scaffold spun from 5 wt% pure PCL showed better cell proliferation than samples from 5 wt% PCL respectively mixed with 5 and 10 wt% BC (Figure 5 comparing S1 and S5 with 5% wt pure PCL). The balance between hydrophilicity and hydrophobicity in the material has been reported to influence the attachment of Saos-2 cells
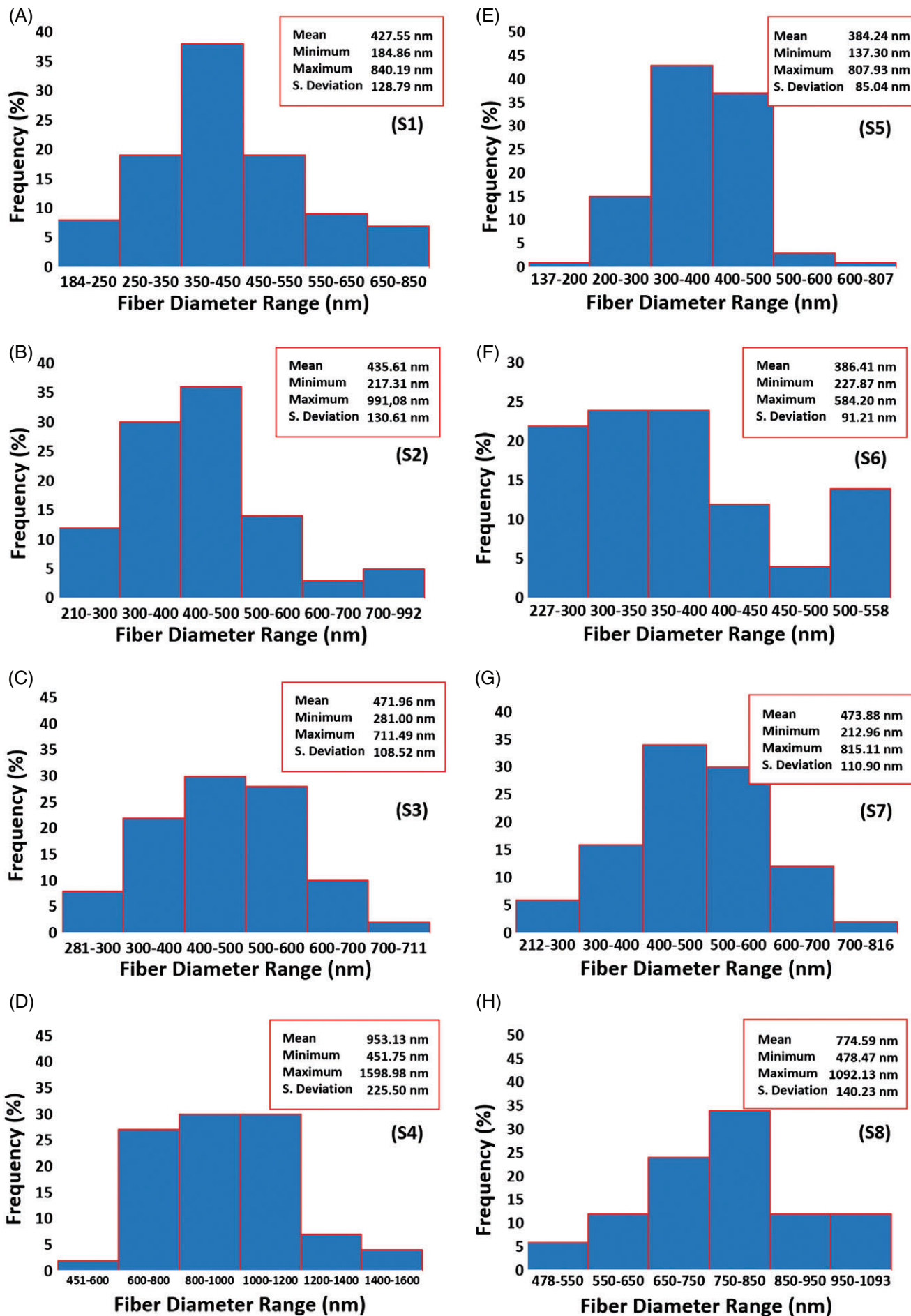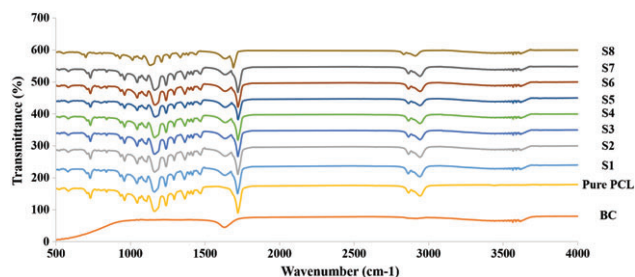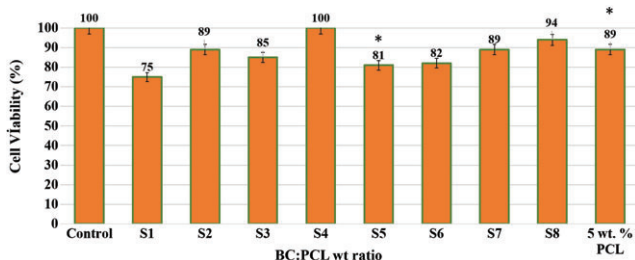
**FIGURE 3** Fibre diameter distribution profile of the samples. A, S1; B, S2; C, S3; D, S4; E, S5; F, S6; G, S7; and H, S8

**FIGURE 4** Fourier transform infrared spectroscopy (FTIR) spectra of pure bacterial cellulose (BC), pure polycaprolactone (PCL), and BC–PCL samples of S1–S8
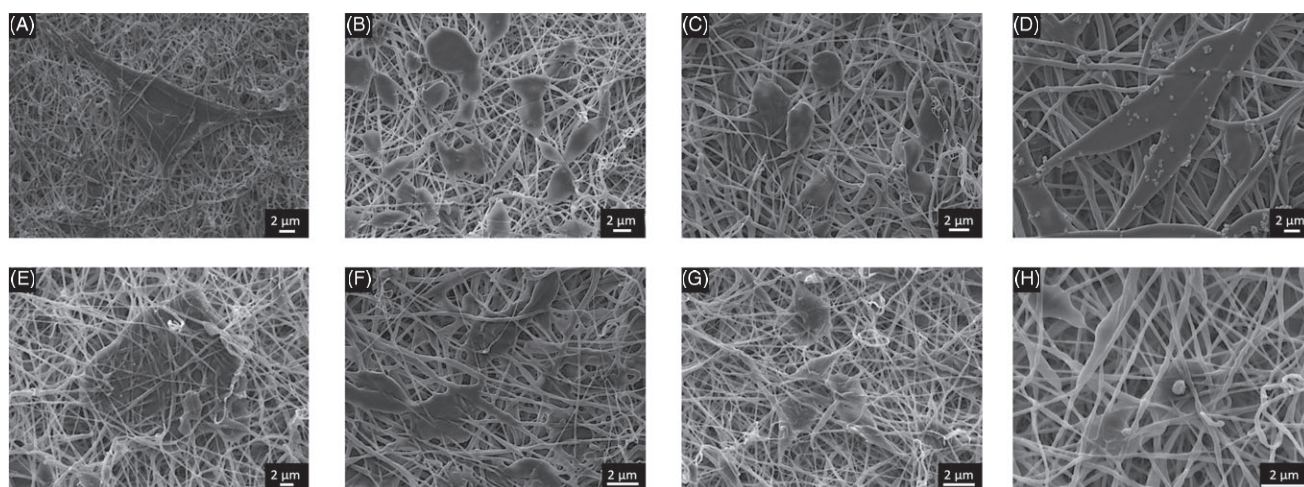


**FIGURE 5** MTT assay shows cell proliferation with respect to a 72-hour culture period of Saos-2 cell line. All sample data are presented relative to the control group (cell suspension cultured in polystyrene plate without scaffold), which was set at 100% (*P value <.05 is significant)

absorption of physiological secretions, allows efficient exchange of nutrients and wastes, and facilitates cell migration as the pores between the polymer network in the scaffold enlarge with the swelling. Ideally, the material should also have a steadily increasing swelling profile that reaches equilibrium without any fluctuations in the absorption, indicating good ability to retain the liquid absorbed. The swelling characteristics of the scaffold samples S1–S8 were determined by immersing the samples in PBS solution at pH 7.4 and 37 °C for 24 hours. All samples were found to swell and expand in PBS within the first 30 minutes of immersion, with S2 scaffolds swelling the most to 393% of original weight (Figure S1). However, over the next 1410 minutes, not all samples were able to retain the water initially absorbed, and scaffolds S1, S2, S5, and S6 showed strong fluctuations in their swelling behaviour. Eventually at 24 hours of immersion, S1 scaffolds with the lowest BC (5 wt%) and PCL (5 wt%) concentrations showed the lowest swelling percentage of 47.4%, whilst S8 scaffolds with the highest BC (10 wt%) and PCL (20 wt%) concentrations showed the highest swelling percentage of 183.3% (Figure S1). This corresponded to the lowest cell viability observed at 75% in S1 scaffolds versus the second highest cell viability of 94% in S8 samples (Figure 6).

The cell–scaffold interaction at 24 hours was also examined by SEM (Figure 6). Cells were found to have started to cover the scaffold and fill the spaces between the nanofibres. Two main cell morphologies were observed: cells along the axial length of nanofibres showed stretched/elongated morphology, with the direction of stretching being anisotropic to the axial direction of the nanofibre; on the other hand, a second cell morphology of oblong or globule-shaped cells was observed at cross-junctions of nanofibres, where cells were covering the spaces bridged by the fibres without any specificity to any axial directions. Of particular interest is the stretched morphology of cells, indicating a cytoskeletal rearrangement that has been reported to activate receptors on the

on the scaffolds.[28] In our study, the varying cell viabilities on scaffolds with different BC:PCL ratios further support this argument. Future study on cell proliferation in scaffolds made of similar BC:PCL ratio (therefore of comparable hydrophilicity) but comprising different morphologies (such as fibre diameter, fibre spacing, and scaffold thickness) would bring a better understanding of the effect of the morphology of the BC:PCL scaffolds on cell proliferation.

In addition, it is useful to discuss cell viability in the context of the swelling/water absorption capability of the scaffolds. Swelling ratio is an important factor in wound-dressing materials. A scaffold with a high swelling ratio enables good liquid



**FIGURE 6** Scanning electron microscopy (SEM) images of Saos-2 cells seeded BC–PCL scaffolds. A, S1; B, S2; C, S3; D, S4; E, S5; F, S6; G, S7; and H, S8. Scale bars: 2 μm. Magnifications: (A) 4000×, (B) 5000×, (C) 5000×, (D) 5000×, (E) 5000×, (F) 8000×, (G) 5000×, and (H) 10 000×

cells, thereby affecting gene expression.[29] Cells appeared to locate close to each other, making for better proliferation and cell–cell communication. In addition, cells were observed to spontaneously progress beneath the surface layer of nanofibres and had started to be embedded into the scaffold, showing positive signs of material biocompatibility. Although no significant difference was observed at 24 hours in the Saos-2 cell behaviour between the 8 samples, we do not exclude the possibility that cell attachment could be different among the samples during earlier hours. For instance, Sombatmankhong et al. has observed comparable Saos-2 cell attachment on all of their scaffold samples at 24 hours, although less Saos-2 cells attached at 4 hours on samples with higher hydrophobicity (tissue-plate polystyrene) versus more hydrophilic scaffolds using poly(3-hydroxybutyrate) and poly(3-hydroxybutyrate-*co*-2-hydroxyvalerate).[30] The effect of the hydrophobic–hydrophilic balance of the BC–PCL scaffolds on initial cell attachment and proliferation is a topic that should be further studied in the future.

## 4 | DISCUSSION

In the present study, we demonstrate 3 findings for the first time: (1) the successful electrospinning of 8 PCL–BC nanofibrous scaffolds with varying BC:PCL ratios; (2) the proliferation of human Saos-2 cells on the composite BC–PCL scaffolds, indicating good biocompatibility for tissue-engineering and wound-healing applications; and (3) the novel use of a hand-held, portable EHD gun that enables point-of-need, in situ production of sophisticated BC–PCL nanofibrous scaffolds, allowing advanced medical attention to be swiftly provided without the need to package and transport the delicate nanofibres.

When considering the potential of BC–PCL scaffolds as an exciting candidate for a novel and idealistic wound dressing in the clinical context, it is useful to examine the process of wound healing itself to highlight its advantages. Wound closure by primary intention involves 4 key stages: haemostasis, inflammation, proliferation, and remodelling. Timing is critically important to wound healing. Most significantly, the timing of wound reepithelialisation can decide the outcome of the healing. So, the use of the portable hand-held EHD gun could allow for the use of enhanced biocompatible scaffolds to be placed onto the wound site in a time-dependent fashion as demanded by the wound-healing process. The electrospinning process can also enhance haemostasis, thus providing another clinical benefit of use. Harnessing the natural non-toxic properties of bacterial cellulose by combining it with the mechanically strong polycaprolactone allows for optimal properties in the microcosm of the cellular environment within the wound. This is particularly important at the inflammation phase of wound healing. Further work to establish the ideal ratio will refine this dressing and its potential further. Fibroblasts are critical in supporting normal

wound healing, involved in key processes such as breaking down the fibrin clot, creating new extra cellular matrix and collagen structures to support other cells associated with effective wound healing, as well as wound contracture. The nano-scale structure of this scaffold seems to suit the fibroblast in terms of attachment and proliferation. The positive findings discovered with embedding, cell proximity, and morphology of the Saos-2 cell line further reinforce the clinical relevance of this work. A dressing that can be accurately moulded and standardised via the EHD gun technique is advantageous not only in terms of wound healing cell attachment but also in practicality and in its consistency through mass production. The PCL–BC scaffolds hold several clinically positive properties that are demonstrated at each stage of the wound-healing process and now, with a unique and sophisticated way of delivery, could be mass produced for the acute medical setting.

## ORCID

*CJ Luo* http://orcid.org/0000-0002-9898-695X

## REFERENCES

1. Norouzi M, Boroujeni SM, Omidvarkordshouli N, Soleimani M. Advances in skin regeneration: application of electrospun scaffolds. *Adv Healthc Mater*. 2015;4(8):1114-1133. https://doi.org/10.1002/adhm.201500001.
2. Guillaume O, Teuschl AH, Gruber-Blum S, Fortelny RH, Redl H, Petter-Puchner A. Emerging trends in abdominal wall reinforcement: bringing bio-functionality to meshes. *Adv Healthc Mater*. 2015;4(12):1763-1789. https://doi.org/10.1002/adhm.201500201.
3. Field FK, Kerstein MD. Overview of wound healing in a moist environment. *Am J Surg*. 1994;167(1A):2S-6S.
4. Kim J, Kim SW, Park S, et al. Bacterial cellulose nanofibrillar patch as a wound healing platform of tympanic membrane perforation. *Adv Healthc Mater*. 2013;2(11):1525-1531. https://doi.org/10.1002/adhm.201200368.
5. Moreira S, Silva NB, Almeida-Lima J, et al. BC nanofibres: in vitro study of genotoxicity and cell proliferation. *Toxicol Lett*. 2009;189(3):235-241. https://doi.org/10.1016/j.toxlet.2009.06.849.
6. Chen YM, Xi T, Zheng Y, et al. In vitro cytotoxicity of bacterial cellulose scaffolds used for tissue-engineered bone. *J Bioactive Compatible Polym*. 2009;24(Suppl. 1):137-145. https://doi.org/10.1177/0883911509102710.
7. Lin N, Dufresne A. Nanocellulose in biomedicine: current status and future prospect. *Eur Polym J*. 2014;59(Suppl. C):302-325. https://doi.org/10.1016/j.eurpolymj.2014.07.025.
8. Leung V, Ko F. Biomedical applications of nanofibers. *Polym Adv Technol*. 2011;22(3):350-365. https://doi.org/10.1002/pat.1813.
9. Rim NG, Shin CS, Shin H. Current approaches to electrospun nanofibers for tissue engineering. *Biomed Mater*. 2013;8(1):014102.
10. Luo CJ, Stoyanov SD, Stride E, Pelan E, Edirisinghe M. Electrospinning versus fibre production methods: from specifics to technological convergence. *Chem Soc Rev*. 2012;41(13):4708-4735. https://doi.org/10.1039/C2CS35083A.
11. Kumbar SG, James R, Nukavarapu SP, Laurencin CT. Electrospun nanofiber scaffolds: engineering soft tissues. *Biomed Mater*. 2008;3(3):034002. https://doi.org/10.1088/1748-6041/3/3/034002.
12. Hiep NT, Lee B-T. Electro-spinning of PLGA/PCL blends for tissue engineering and their biocompatibility. *J Mater Sci Mater Med*. 2010;21(6):1969-1978. https://doi.org/10.1007/s10856-010-4048-y.

13. Chong EJ, Phan TT, Lim IJ, et al. Evaluation of electrospun PCL/gelatin nanofibrous scaffold for wound healing and layered dermal reconstitution. *Acta Biomater*. 2007;3(3):321-330. https://doi.org/10.1016/j.actbio.2007.01.002.

14. Kim BJ, Cheong H, Choi E-S, et al. Accelerated skin wound healing using electrospun nanofibrous mats blended with mussel adhesive protein and polycaprolactone. *J Biomed Mater Res A*. 2017;105(1):218-225. https://doi.org/10.1002/jbm.a.35903.

15. Kim CH, Khil MS, Kim HY, Lee HU, Jahng KY. An improved hydrophilicity via electrospinning for enhanced cell attachment and proliferation. *J Biomed Mater Res*. 2006;78B(2):283-290. https://doi.org/10.1002/jbm.b.30484.

16. Sofokleous P, Stride E, Bonfield W, Edirisinghe M. Design, construction and performance of a portable handheld electrohydrodynamic multi-needle spray gun for biomedical applications. *Mater Sci Eng C Mater Biol Appl*. 2013;33(1):213-223. https://doi.org/10.1016/j.msec.2012.08.033.

17. Lau WK, Sofokleous P, Day R, Stride E, Edirisinghe M. A portable device for in situ deposition of bioproducts. *Bioinspir Biomim Nanobiomater*. 2014;3(2):94-105. https://doi.org/10.1680/bbn.13.00030.

18. Mosmann T. Rapid colorimetric assay for cellular growth and survival: application to proliferation and cytotoxicity assays. *J Immunol Methods*. 1983;65(1–2):55-63.

19. Fong H, Chun I, Reneker DH. Beaded nanofibers formed during electrospinning. *Polymer*. 1999;40(16):4585-4592.

20. Cloupeau M, Prunetfoch B. Electrostatic spraying of liquids – main functioning modes. *J Electrostat*. 1990;25(2):165-184.

21. Yang Z, Chen S, Hu W, et al. Flexible luminescent CdSe/bacterial cellulose nanocomoposite membranes. *Carbohydr Polym*. 2012;88(1):173-178. https://doi.org/10.1016/j.carbpol.2011.11.080.

22. Elzein T, Nasser-Eddine M, Delaite C, Bistac S, Dumas P. FTIR study of polycaprolactone chain organization at interfaces. *J Colloid Interface Sci*. 2004;273(2):381-387. https://doi.org/10.1016/j.jcis.2004.02.001.

23. Lee S, Leach MK, Redmond SA, et al. A culture system to study oligodendrocyte myelination processes using engineered nanofibers. *Nat Methods*. 2012;9(9):917-922. https://doi.org/10.1038/nmeth.2105.

24. Hsia HC, Nair MR, Mintz RC, Corbett SA. The fiber diameter of synthetic bioresorbable extracellular matrix influences human fibroblast morphology and fibronectin matrix assembly. *Plast Reconstr Surg*. 2011;127(6):2312-2320. https://doi.org/10.1097/PRS.0b013e3182139fa4.

25. Badami AS, Kreke MR, Thompson MS, Riffle JS, Goldstein AS. Effect of fiber diameter on spreading, proliferation, and differentiation of osteoblastic cells on electrospun poly(lactic acid) substrates. *Biomaterials*. 2006;27(4):596-606. https://doi.org/10.1016/j.biomaterials.2005.05.084.

26. Kim J-E, Noh K-T, Yu H-S, Lee H-Y, Jang J-H, Kim H-W. A fibronectin peptide-coupled biopolymer nanofibrous matrix to speed up initial cellular events. *Adv Eng Mater*. 2010;12(4):B94-B100. https://doi.org/10.1002/adem.200980008.

27. Zhang YZ, Ouyang HW, Lim CT, Ramakrishna S, Huang ZM. Electrospinning of gelatin fibers and gelatin/PCL composite fibrous scaffolds. *J Biomed Mater Res B Appl Biomater*. 2005;72B(1):156-165.

28. Yang X, Zhao K, Chen G-Q. Effect of surface treatment on the biocompatibility of microbial polyhydroxyalkanoates. *Biomaterials*. 2002;23(5):1391-1397.

29. Curtis A, Wilkinson C. Topographical control of cells. *Biomaterials*. 1997;18(24):1573-1583.

30. Sombatmankhong K, Sanchavanakit N, Pavasant P, Supaphol P. Bone scaffolds from electrospun fiber mats of poly(3-hydroxybutyrate), poly(3--hydroxybutyrate-co-3-hydroxyvalerate) and their blend. *Polymer*. 2007;48(5):1419-1427. https://doi.org/10.1016/j.polymer.2007.01.014.

## SUPPORTING INFORMATION

Additional Supporting Information may be found online in the supporting information tab for this article.